JOURNAL OF MATERIALS SCIENCE **39** (2004) 2663–2674

Preparation of helical TiO_2/CMC microtubes and pure helical TiO_2 microtubes

S. MOTOJIMA, T. SUZUKI, Y. NODA, A. HIRAGA, S. YANG, X. CHEN
Department of Applied Chemistry, Faculty of Engineering, Gifu University, Gifu 501-1193, Japan
E-mail: motojima@apchem.gifu-u.acjp

H. IWANAGA, T. HASHISHIN
Department of Material Science and Engineering, Faculty of Engineering, Nagasaki University, Nagasaki 852-8521, Japan

Y. HISHIKAWA
CMC Technology Development Co., Ltd., Kakamigahara, Gifu 509-0108, Japan

Helical TiO_2/CMC (carbon microcoils) microtubes and helical TiO_2 microtubes were obtained by making TiO_2 layer coatings on the surface of CMC templates using a sol-gel and chemical vapor deposition (CVD) processes. The preparation conditions, morphologies and some properties were examined. Uniform TiO_2 (anatase) layers were obtained on the CMC templates by a CVD process using vapor phase hydrolysis of titanium tetra-isopropoxide at 300°C followed by heat treatment in N_2 or by calcination in air at 500–650°C. The helical TiO_2/CMC microtubes showed good photocatalytic activity. It was considered that the helical structure activated and enhanced the photocatalytic activity of TiO_2, probably caused by the generation of inductive microelectric current induced by the irradiation of UV light, resulting in the generation of micromagnetic fields around the tubes.

1. Introduction

Materials with a microcoiled structure are potential candidates for the absorbers of electromagnetic (EM) waves, for tunable micro-devices, micro-sensors, micro-actuators, micro-antenna, hydrogen storage materials, electrode materials, activation catalysts for microorganisms, active molds for the preparation of α-helix proteins, etc. Accordingly, many researchers have been trying to prepare materials with a 3D-helical/spiral structure. Some researchers reported the vapor growth of coiled fibers of carbon [1–4], SiC [5–7], Si_3N_4 [7–11] and SiO_2 [12]. However, the growth of these coiled fibers from the vapor phase were mostly accidental and the reproducibility was very poor. Preparation of chiral and helical fibers of SiO_2 [13, 14] and transition-metal oxide [15] using the sol-gel transcription process were also reported.

We prepared regularly microcoiled carbon fibers (referred to as "carbon microcoils" or "CMC" hereafter) with high reproducibility by the catalytic pyrolysis of acetylene containing a small amount of sulfur or phosphorus impurity, and reported the preparation conditions, morphologies, and some properties of the products [16–21]. We also prepared various ceramic microcoils and/or microtubes, such as SiC [22], TiC [23, 24], ZrC [25], and NbC [26] by the vapor phase metallizing of the carbon microcoils, with full preservation of the coiling morphology. Furthermore, we prepared the microcoils/microtubes of TiN [27] and NbN [28] by the vapor phase metallizing/nitriding of the carbon microcoils or by nitriding of metal carbide coils in a nitrogen atmosphere at 800–1200°C.

Titanium dioxide (TiO_2) of anatase phase has been intensively investigated because of its notable photocatalytic activity. On the other hand, the carbon microcoils have very high absorption ability of EM waves in the GHz region. Accordingly, we can expect that helical TiO_2/CMC composite microtubes and pure helical TiO_2 microtubes may be potential candidates for novel photocatalytic materials, EM absorbers, electrical microdevices, etc. For the preparation of anatase-phase TiO_2 layers, which has higher photocatalytic activity than that of the rutile-phase, a variety of preparation processes, such as sol-gel [29, 30], CVD, spray pyrolysis [31, 32], electric plating processes [33, 34], etc. have been investigated. TiO_2 pillar crystals [35, 36] or nanotubes [37, 38] have also been prepared. However, TiO_2 fiber or tubes of microcoiled structure have never been prepared so far. Recently, we have found that uniform TiO_2 layers of anatase-phase were formed on the surface of CMC templates by a sol-gel process or a CVD process using titanium tetra-isopropoxide (TIPO) as a Ti source and helical TiO_2 microtubes could be easily obtained [39, 40].

In this study, helical TiO_2/CMC composite microtubes (refer to as "helical TiO_2/CMC microtubes"

hereafter) and pure helical TiO_2 microtubes (refer to as "helical TiO_2 microtubes" hereafter) were obtained by the coating of TiO_2 layers on the CMC templates using the sol-gel and CVD processes. The preparation conditions, morphologies and some properties were examined in detail.

2. Experimental

2.1. Source carbon microcoils

Carbon microcoils (CMC) were prepared by the Ni-catalyzed pyrolysis of acetylene at 740–800°C. A detailed preparation procedure was described in Ref. [17]. The CMC were generally very regular and double-helically coiled with a constant coil diameter of 2–10 μm, coil length of 0.2–5 mm, without a coil gap. The representative morphology of the CMC used as the template is shown in Fig. 1.

2.2. TiO_2 coating and calcinating processes

The formation of TiO_2 layer on the CMC templates was carried out using a sol-gel process or a CVD process. In both processes, titanium tetra-isopropoxide (refer to as "TIPO" hereafter) was used as the Ti source. In the sol-gel process, ethyl alcohol solution (3×10^{-6} m^3) containing TIPO and CMC (10 mg) was mixed with ethyl alcohol solution (6×10^{-6} m^3) containing a 2 M HCl (2×10^{-8} m^3), and the mixture was stirred by using supersonic bath, aged (2 h), concentrated under vacuum, dried, and heat-treated or calcinated. The addition amount of TIPO was 2–8 $\times$ 10^{-7} m^3, and the concentration ratio was 25–100% (full drying). In the CVD process, the CMC was coated with TiO_2 layers using a gas mixture of TIPO + H_2O + N_2 at 300°C for 2 h using a rotating CVD reactor as shown in Fig. 2. The rotating speed was fixed at 25 rpm. The TiO_2-coated CMC was then heat-treated in N_2 atmosphere or calcined in air atmosphere at 500–800°C for 2 h. The amount of TiO_2 deposited on the surface of CMC was estimated from the ignition loss obtained at 500°C in air using a TG apparatus.

2.3. Measurement of photocatalytic activity

UV light (365 nm, 4 W) was irradiated onto 20 g/m^3 Methyl Orange (refer to as "MO" hereafter) aqueous solution containing 0.03 g sample (TiO_2/CMC, etc.), and the reactor volume was 1.0×10^{-4} m^3. The degree of decomposition of the MO molecules was measured by an UV spectrometer. The photocatalytic activity of the CVD–coated helical TiO_2/CMC and TiO_2 microtubes were estimated by the intensity ratio of absorbance of 460 nm of the MO molecule, A/Ao, where A is the intensity of 460 nm for the addition of sample and Ao is without addition.

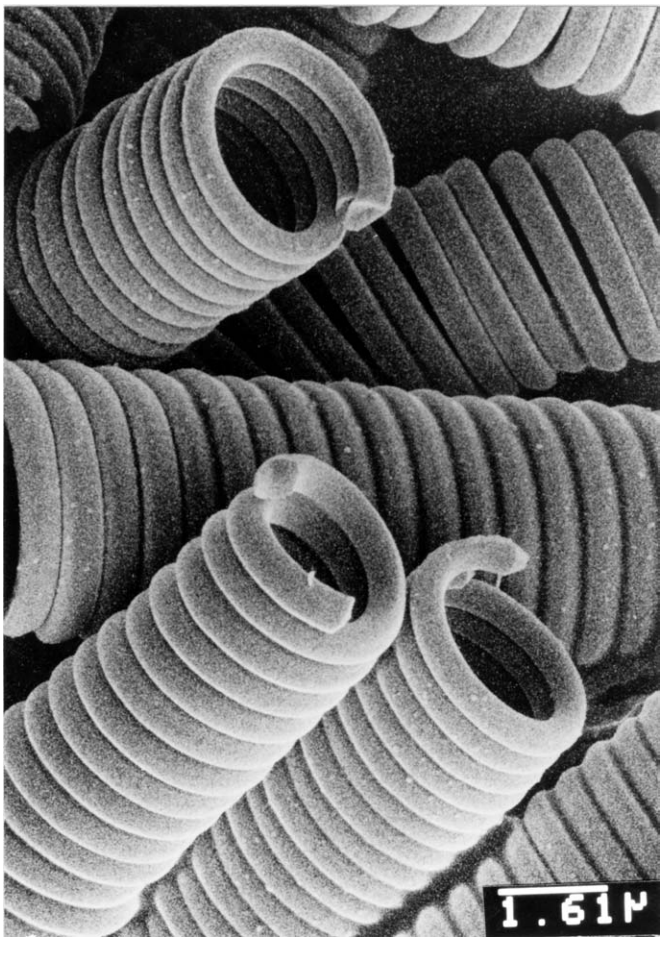

Figure 1 Representative carbon microcoils used as a template.

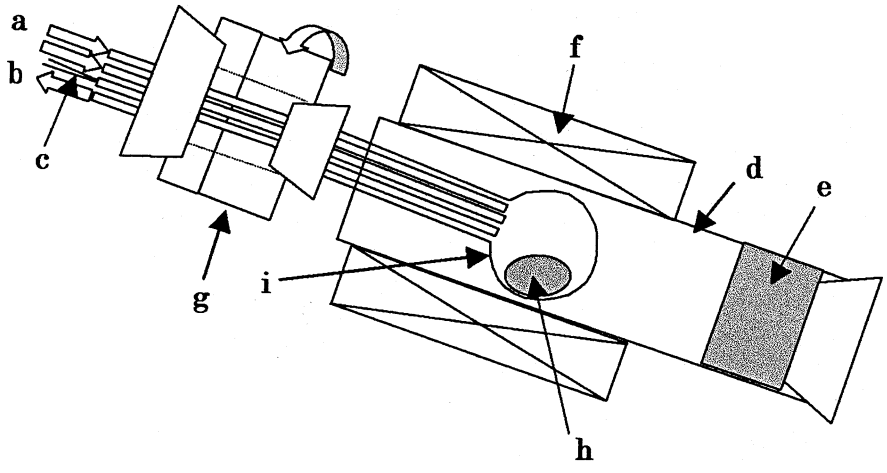

Figure 2 CVD apparatus: (a) Source gas (Ti(O-iso $C_3H_7)_4$, (b) gas outlet, (c) CA thermocouple, (d) furnace, (e) brick, (f) heater, (g) rotation disk (25 rpm), (h) carbon microcoils and (i) reaction tube (quartz, 40 mm i.d.).

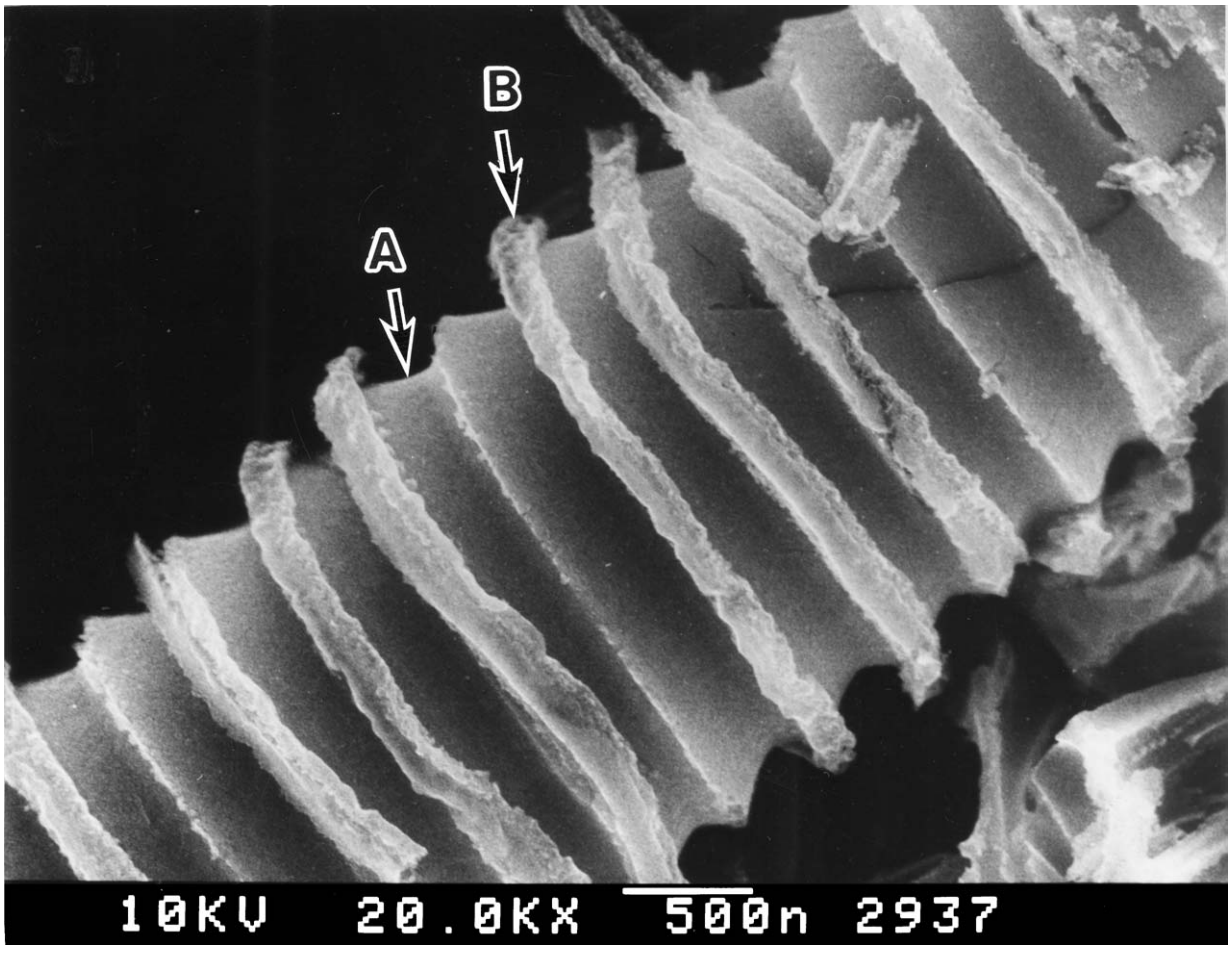

Figure 3 (a) Helical TiO_2 microtubes and (b) helical TiO_2 microtubes with thin TiO_2 microcoils on the outer surface obtained by a sol-gel process. TIPO: 0.2×10^{-6} m^3 (6.6×10^{-6} m^3/g-CMC).

3. Results and discussion

3.1. Preparation of helical TiO_2 mictotubes by sol-gel process

Fig. 3 shows the SEM image of the helical TiO_2 microtubes obtained by the TiO_2 layer coating on the surface of CMC using a sol-gel process (TiO_2/CMC microtube) followed by the calcination at 500°C in air, in which the addition amount of TIPO was 0.2×10^{-6} m^3. The CMC template was burned out in the calcination process and 'negative coiling patterns' were observed on the surface of the calcined product (arrow A). The color of TiO_2/CMC microtubes changed from gray or dark gray to the color of pure TiO_2 tubes with outer negative coiling patterns, which is pale-yellowish white. These kind of negative patterns, in which some substances were evacuated or disappeared and only pores with certain shapes remained, were also observed in negative whiskers or crystals [41–44]. The curved inner smooth surface (arrow A) was of the TiO_2 coating layers deposited on the inner surface of the CMC templates and

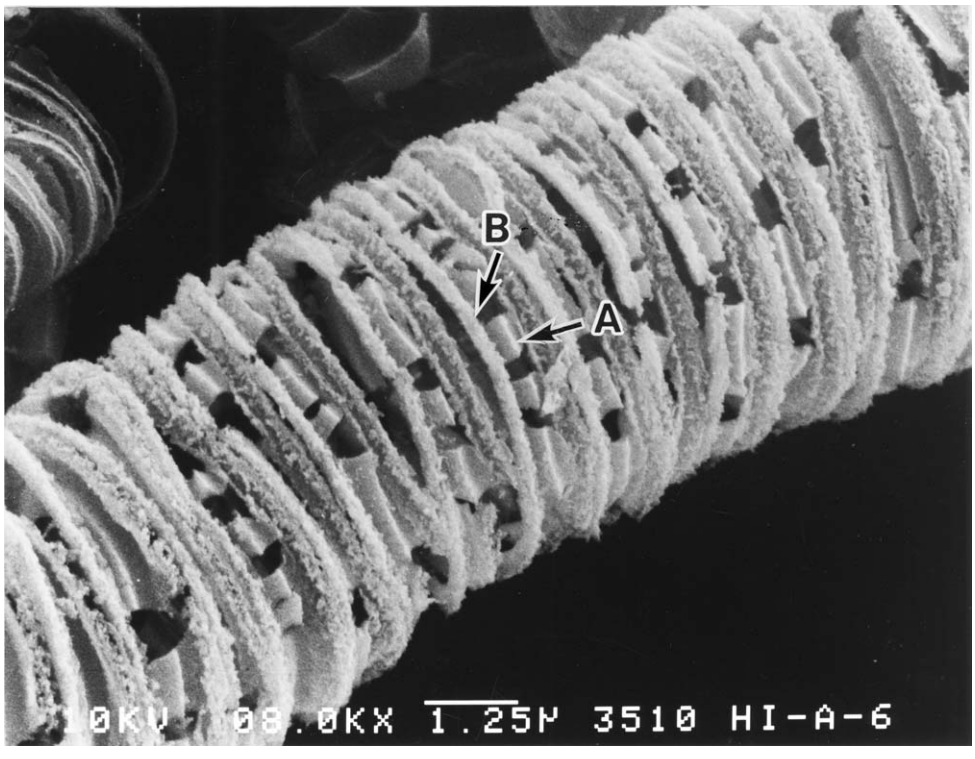

Figure 4 TiO_2 microcoils. TIPO: 0.4×10^{-6} m^3 (40×10^{-6} m^3/g-CMC).

a central straight hollow tube was present in the tube axis although it cannot be observed in this figure. That is, the helical TiO_2 microtubes with helical coiling patterns on the outer surface were formed. On the other hand, arrow B indicates the TiO_2 fibers deposited on a channel between two adjacent fibers from which CMC were constructed. Fig. 4 shows the TiO_2 microcoils obtained by the addition of 0.4×10^{-6} m^3 of TIPO. Uniform TiO_2 layers, such as observed in Fig. 3, which was formed in the inner surface of CMC templates was ruptured here and there (arrow A), while continuous TiO_2 fibers (coils) are formed (arrow B). Fig. 5 shows the continuous double helical TiO_2 microcoils obtained by using 0.8×10^{-6} m^3 TIPO.

A formation model of the helical TiO_2 microcoils is shown in Fig. 6. The inner diameter of a pore (tube) which is present through the coil axis of regular CMC templates is several hundred nm to several μm. If the concentration of TIPO is small, the viscosity of the solution is small and the TIPO solution can easily invade into a thin pore (known as the capillary phenomenon) and form TiO_2 layers in the inner pore surface of the CMC as shown in Fig. 6a. On the other hand, if the concentration of TIPO is too much, entry of TIPO solution into the central thin pore is suppressed and thus TiO_2 fibers (coils) form only on the outer surface, especially on a channel present between adjacent two fibers (coils) as shown in Fig. 6b.

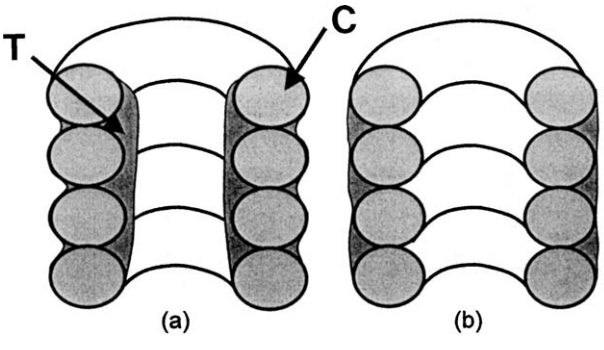

Figure 6 Deposition mechanism of TiO_2 layers on the CMC template by a sol-gel process: C) CMC template, T) TiO_2 layers: (a) Low TIPO concentration ($<0.3 \times 10^{-6}$ m^3) and (b) high TIPO concentration ($>0.3 \times 10^{-6}$ m^3).

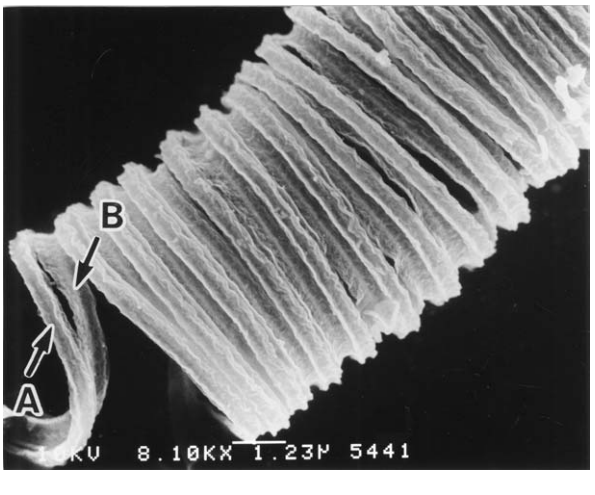

Figure 5 TiO_2 double microcoils. TIPO: 0.8×10^{-6} m^3 (26×10^{-6} m^3/g-CMC).

3.2. Preparation of helical TiO_2/CMC microtubes and pure TiO_2 microtubes by CVD process

Fig. 7 shows the ruptured cross section of the TiO_2-coated CMC (helical TiO_2/CMC microtubes). It can be seen that the uniform TiO_2 layer was formed on the

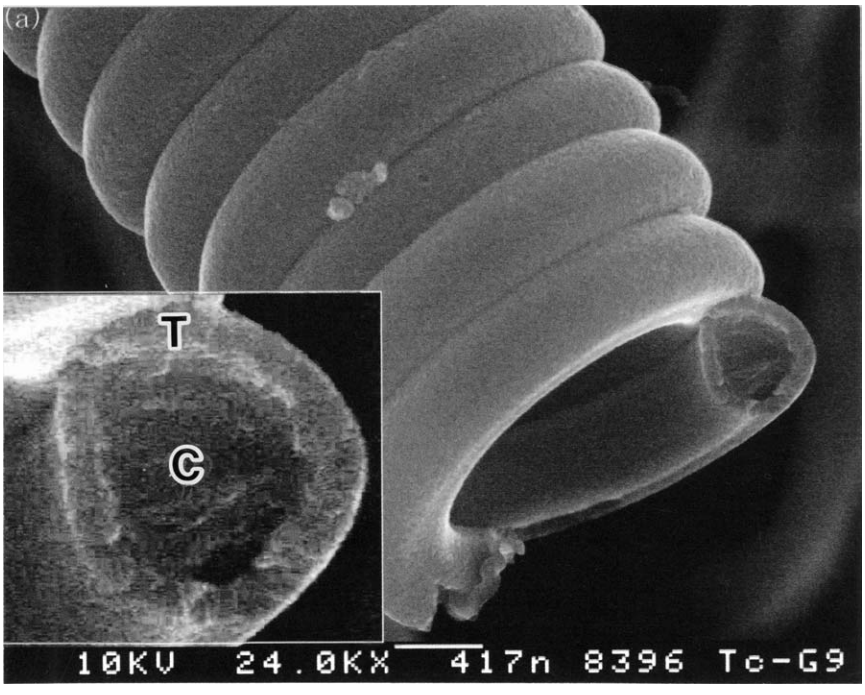

Figure 7 Helical TiO_2/CMC microtubes: C) Carbon microcoils (template), T) TiO_2 layers.

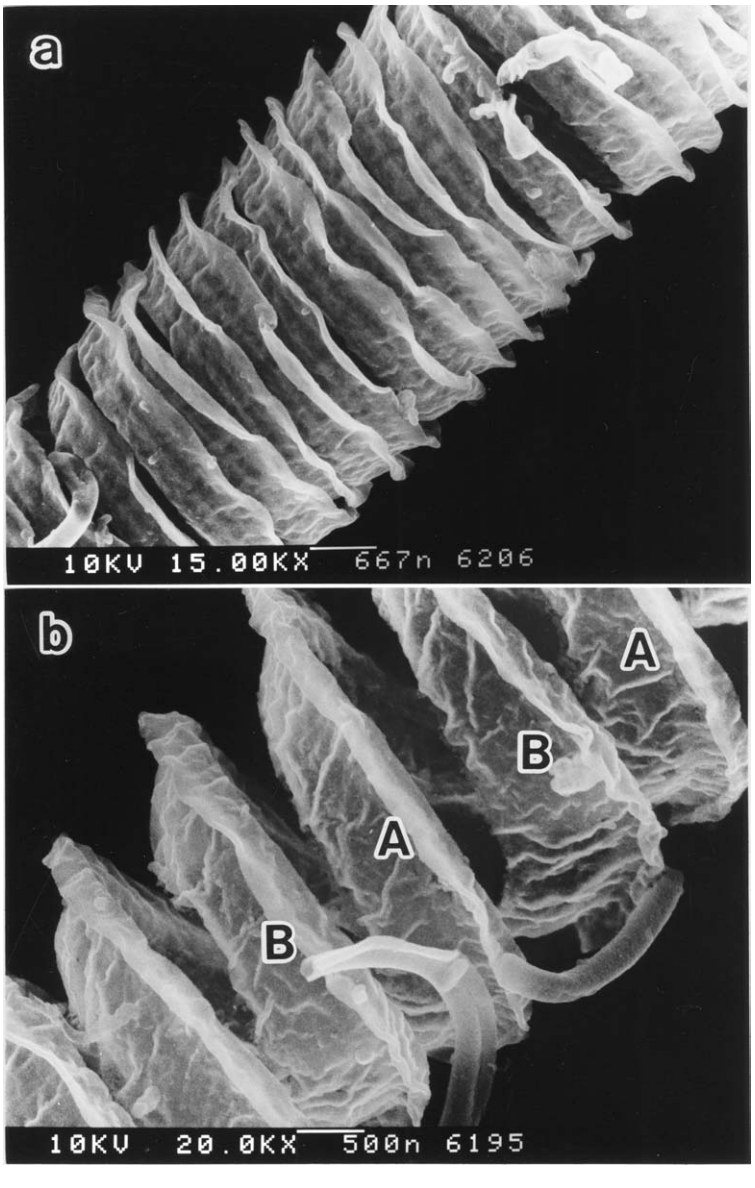

Figure 8 (a) Single helical TiO_2 microcoils obtained using CMC template with flat fiber cross-section and (b) the enlarged view. A and B indicates the double coils.

surface of the CMC. The thickness of the TiO_2 layers is about 200 nm. Using the CVD process, very uniform TiO_2 layers were generally formed on the surface of the CMC template. The color of obtained TiO_2/CMC microtube was gray to dark gray. Some oxygen-containing functional groups, such as hydroxyl, ketone, carboxyl group, are present on the surface of the CMC templates [45]. It is considered that TIPO molecules are partly hydrolyzed in the vapor phase and the formed $TiO_x(O\text{-}iPr)_y(OH)_z$ molecules are then adsorbed on the surfaces of the CMC templates and react with the oxygen-containing groups to form the adherent uniform thin layers with a quasi-liquid phase and finally further hydrolyzed and calcined to form TiO_2 layers. Fig. 8 shows the double (A and B) helical TiO_2 microcoils with thin and wrinkled TiO_2 films, in which the regularly-coiled flat CMC with a flat or rectangular fiber cross section were used as the template. Fig. 9 shows a single helical TiO_2 microtube with a thin TiO_2 layer with a thickness of 100 nm and with a large coil gap. The surface of the TiO_2 tubes was very smooth and no crack was observed among the TiO_2 layers. Fig. 10 shows double helical TiO_2 microstubes (hollow coils) with a TiO_2 layer thickness of 350 nm. The color of the pure TiO_2 microtube was pale-yellowish white. Some cracks are observed, probably caused by the difference in thermal expansion of the CMC templates and TiO_2 layers during the calcination process.

Fig. 11 shows the effect of TIPO gas flow rate on the weight increase and thickness of the TiO_2 layers, in which reaction time was fixed at 2 h. It can be seen that the thickness of the TiO_2 layers increased linearly with increasing TIPO gas flow rate and attained a constant value of 120 nm (60 nm/h) at 4×10^{-6} m^3/min. That is, the thickness of the TiO_2 layers can be controlled by controlling the TIPO flow rate. Fig. 12 shows the effect of gas flow rates of TIPO and H_2O on the yield of helical TiO_2/CMC microcoils, in which the total N_2 gas flow rate was fixed at 1.6×10^{-3} m^3/min. It can be seen that a high yield of regular helical TiO_2/CMC

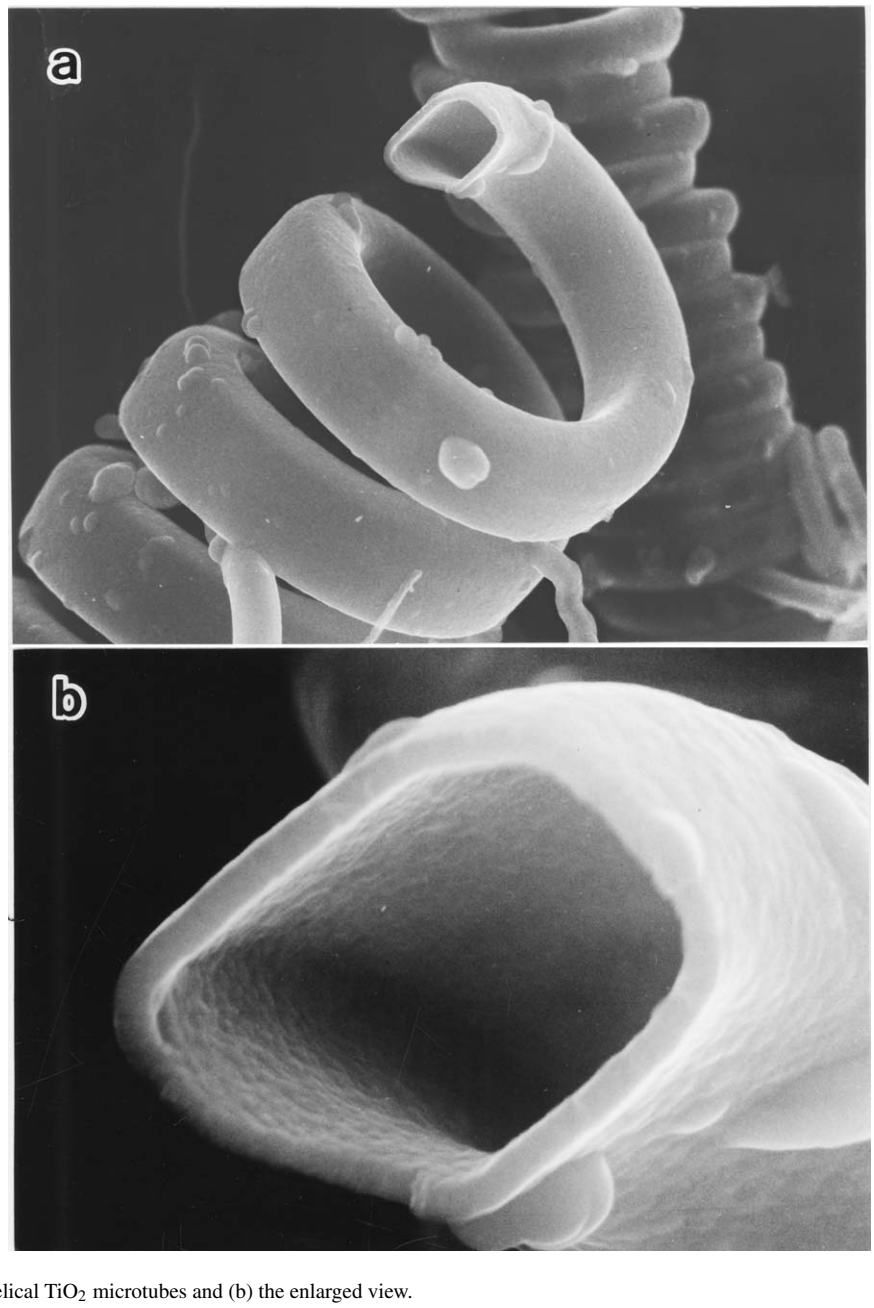

Figure 9 (a) Single helical TiO_2 microtubes and (b) the enlarged view.

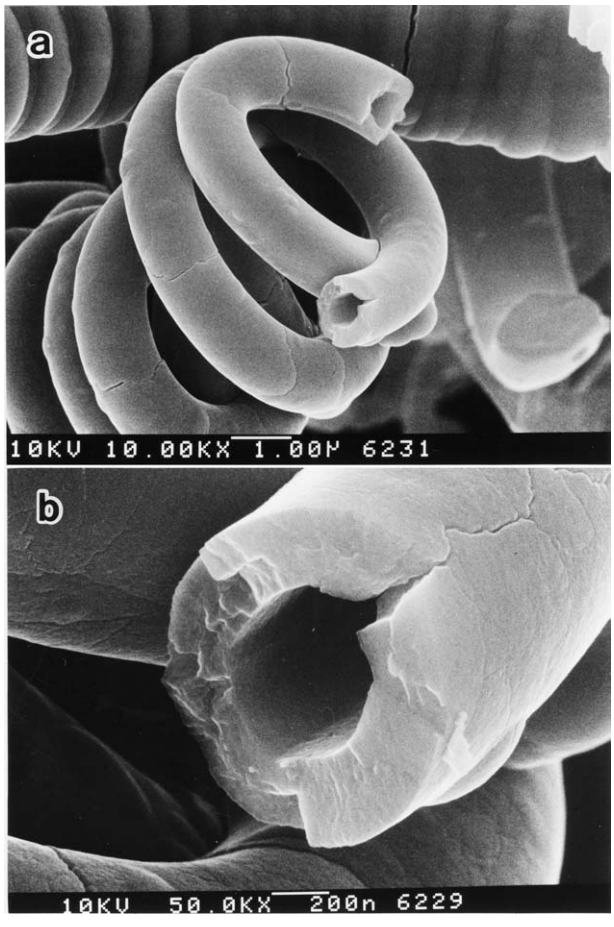

Figure 10 (a) Double helical TiO_2 microtubes and (b) the enlarged view.

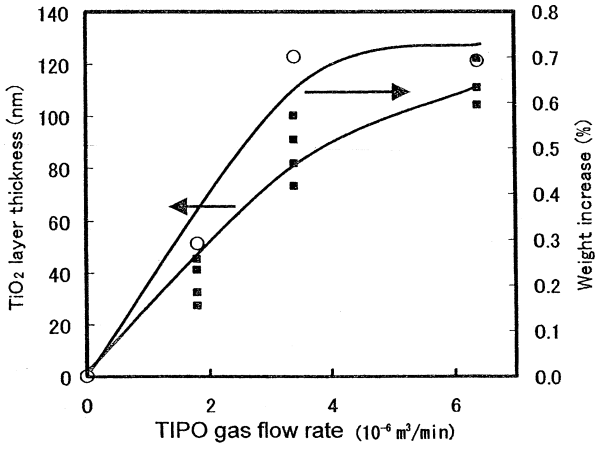

Figure 11 Effects of TIPO gas flow rate on the TiO_2 layer thickness and weight increase: (○) Thickness of TiO_2 layer, (■) weight increase by the deposition of TiO_2.

microcoils was obtained at the TIPO gas flow rate of 6.4×10^{-6} m^3/min and H_2O gas flow rate of 6.9–13.9×10^{-6} m^3/min. Higher gas flow rates of the TIPO or H_2O resulted in the formation of TiO_2 powder. It was observed that the N_2 flow rate also affected the deposition patterns of the TiO_2 films. No uniform and discontinuous TiO_2 layers were deposited at the N_2 flow rate higher than 2.6×10^{-3} m^3/min, while powder-like TiO_2 was deposited at lower than 1.1×10^{-3} m^3/min, probably caused by higher concentration of TIPO in total gas flow resulting in a higher nucleation rate of TiO_2 grains. The optimum gas flow rates for obtaining

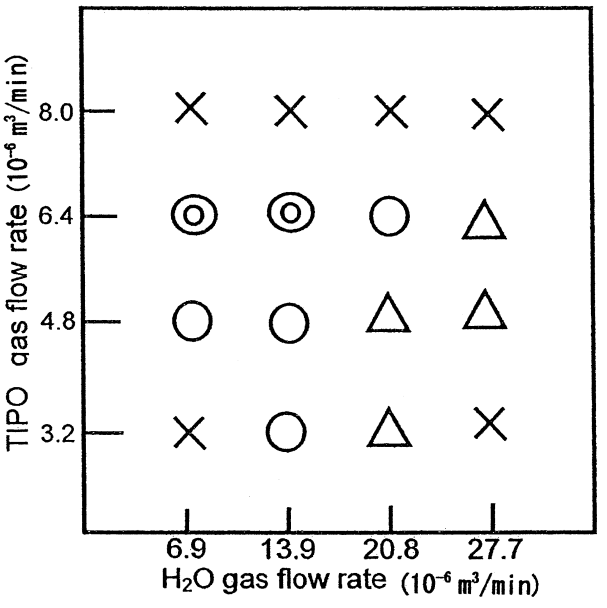

Figure 12 Effect of TIPO and H_2O gas flow rates on the yield of helical TiO_2 microtubes: (◎) >70%, (○) 70–50%, (□) 20–50%, (×) <20%.

the TiO_2-coated CMC with uniform TiO_2 layers and high yield were as follows; TIPO = 6.4×10^{-6} m^3/min, $H_2O = 1.39 \times 10^{-5}$ m^3/min, and total gas flow rate = 1.6×10^{-3} m^3/min. The formed TiO_2 layers formed on the surface of the source CMC template strictly transcribed the coiling morphology of the template. Fig. 13 shows various interesting morphologies of the ruptured cross section of helical TiO_2 microtubes. These interesting morphologies were also derived from that of the original CMC template.

3.3. Microstructure

Fig. 14 shows the XRD patterns of the helical TiO_2 microtubes obtained by CVD process at various calcinating temperatures. It can be seen that the main peaks for the sample obtained at 500°C correspond to the anatase phase and no peaks for the rutile phase are observed. Small peaks corresponding to the rutile phase as well as large peaks of the anatase phase can be seen for the sample obtained at 650°C, and large peaks of rutile at 800°C. Table I shows the density, specific surface area and lattice constants of the helical TiO_2 microtubes obtained by the CVD process. The specific surface area of the helical TiO_2 microtubes was 1.4 m^2/g while the source CMC was about 100 m^2/g, indicating it had a very dense microstructure. Fig. 15 shows the TEM image and electron diffraction patterns of the helical TiO_2 microtubes obtained by the CVD process, in which

TABLE I Physical properties of helical TiO_2 microtubes

Sample	Density (kg/m^3)	Specfic surface area (m^2/g)	Lattice constants (nm)	
			a	*c*
Helical TiO_2 tube	4020	1.4	0.379	0.970
Commercial TiO_2 powder	4070	10.1	0.378	0.966

calcination temperature was 650°C. It can be seen that a pore is developed through the fiber axis. The electron diffraction patterns showed distinct Debye-Sherrer rings suggesting that this helical TiO_2 microtubes has a fine crystalline structure.

3.4. Photocatalytic activity

Fig. 16 shows UV light (365 nm) absorption by the Methyl-Orange (MO) solution containing the helical TiO_2/CMC microtubes obtained by the CVD process. It can be seen that the UV absorption by the MO molecules decreased with increasing irradiation time, indicating a decrease in MO molecule concentration due to the photocatalytic decomposition. The ratio of UV absorbance at 460 nm wavelength of the sample compared to that of the sample without addition was estimated for evaluation of the catalytic activity. Fig. 17 shows the UV absorption ratio (A/Ao) of the as-grown CMC and helical TiO_2/CMC microtubes which were heat-treated at different temperatures in N_2 atmosphere. It can be seen that the highest absorption ratio was obtained for the sample heat-treated at 600–700°C, indicating high photocatalytic activity. The as-grown CMC and heat-treated CMC also absorbed the UV to some extent, probably caused mainly by absorption by MO molecules rather than by their decomposition but absorption of MO molecules. The sample heat-treated at 800°C resulted in low absorption ratio, probably caused by higher rutile content as shown by XRD patterns (see Fig. 15). Also, it can be seen that the absorption ratio of the helical TiO_2/CMC composite microtubes

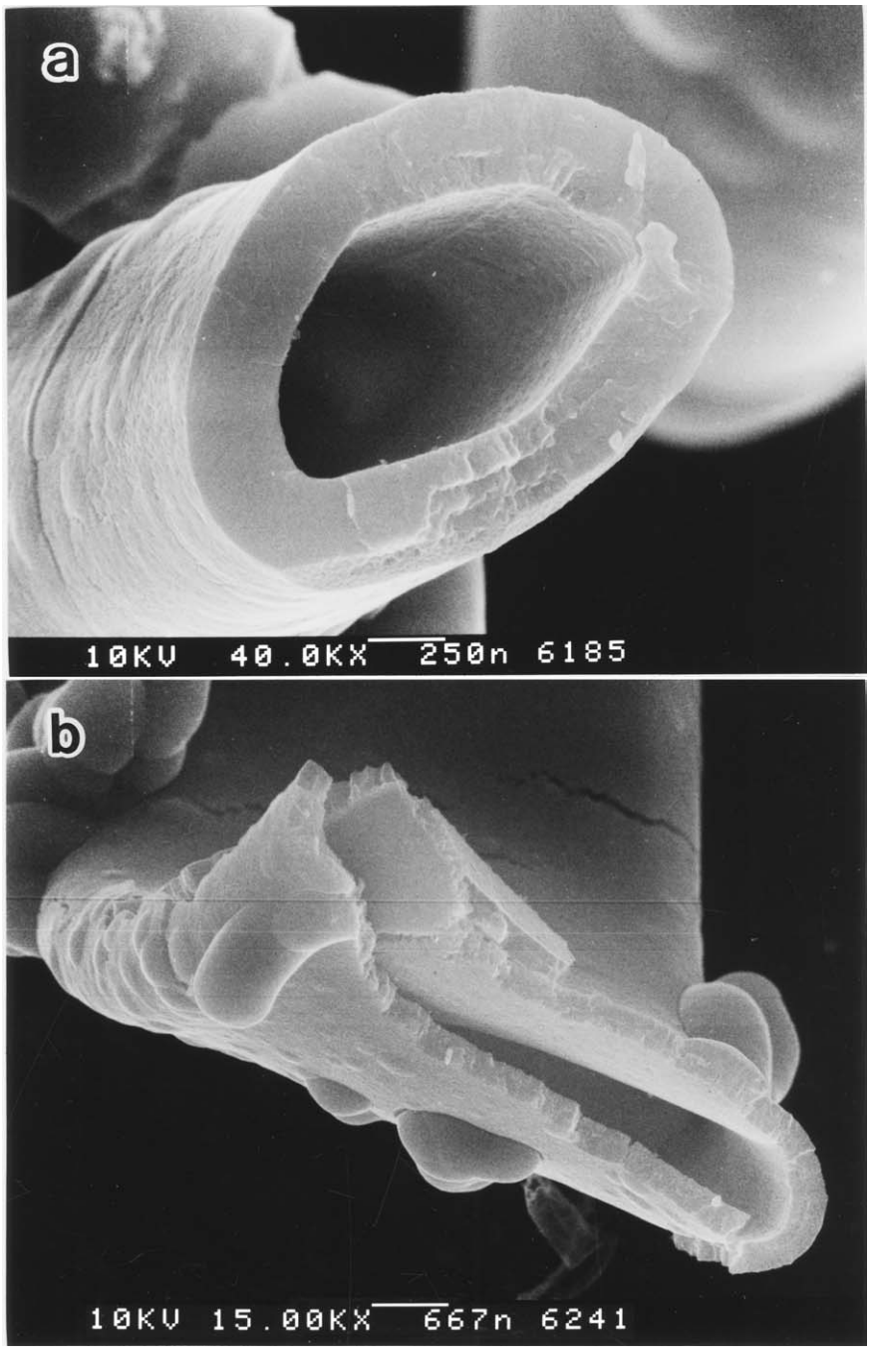

Figure 13 Morphologies of ruptured cross-sections of helical TiO_2 microtubes: (a) Elliptical, (b) ribbon-like, (c) cubic and (d) triangle. (*Continued*)

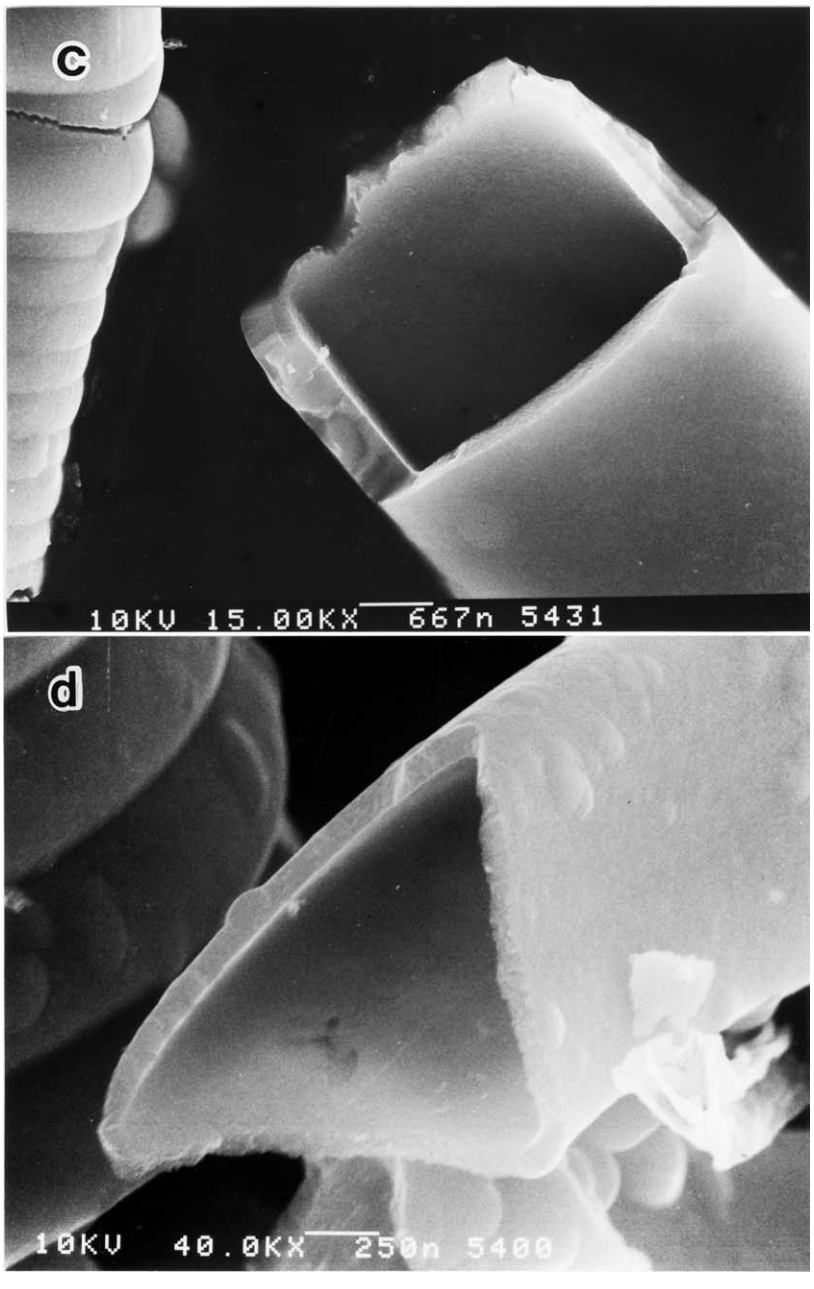

Figure 13 (*Continued*).

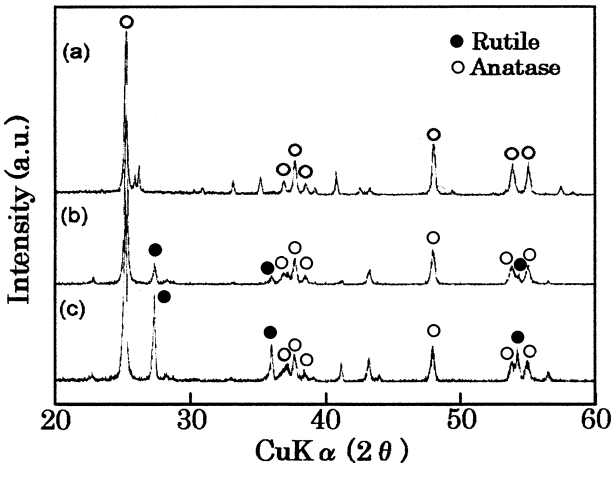

Figure 14 XRD patterns of the helical TiO_2 microtubes obtained at different calcinating temperatures. Calcinating temperature: (a) 500°C, (b) 650°C and (c) 800°C.

was outstandingly higher than that of the commercial TiO_2 powder, indicating very high photocatalytic activity of the helical TiO_2/CMC microtubes. Fig. 18 shows the absorption ratio of the helical TiO_2 microtubes obtained at different calcinations temperatures. It can be seen that the highest absorption ratio was obtained for the sample calcined at 650°C, while no absorption was observed for 800°C, probably caused by the increase of the rutile phase. However, these photocatalytic activites of the helical TiO_2 microtubes are smaller than that of the commercial TiO_2 powder, probably caused by the higher crystallinity and higher rutile phase content. Berry *et al.* reported that TiO_2 with mixed phase of anatase/rutile = 70/30 (%) showed the highest photocatalytic activity for the oxidation of organic molecules [46]. The XRD and absorption ratio (photocatalytic activity) results suggest that this optimum anatase/rutile ratio may

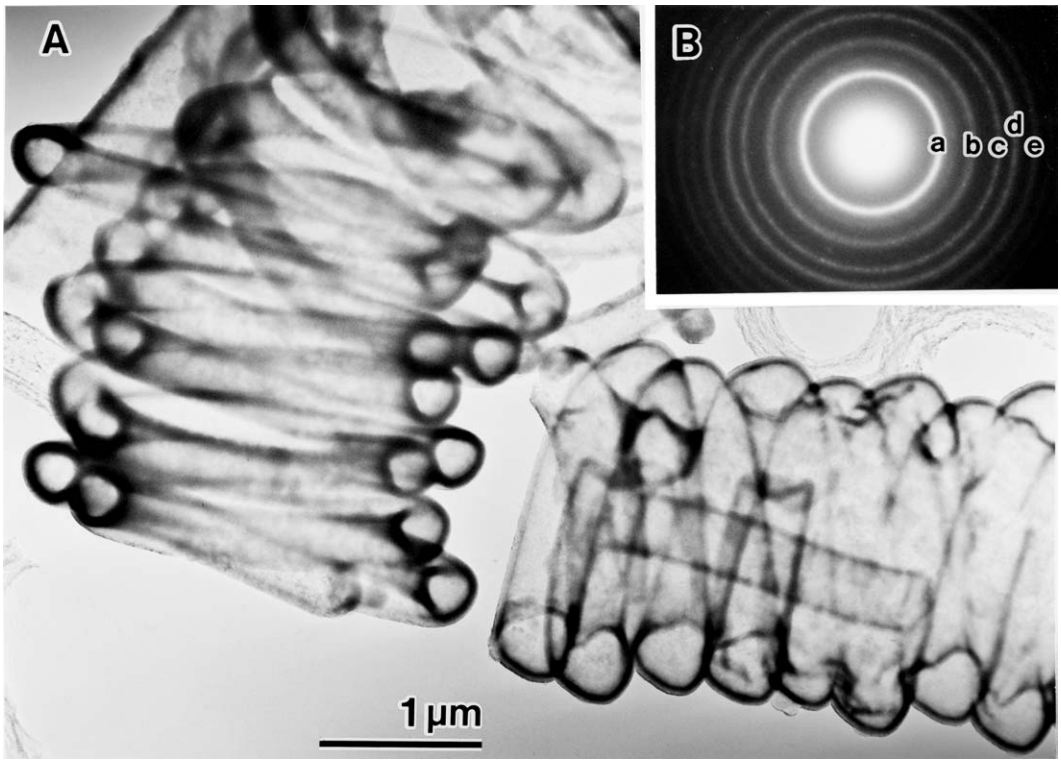

Figure 15 (A) TEM image and (B) electron diffraction patterns of helical TiO_2 microtubes obtained by a CVD process: (a) (101), (b) (004), (c) (200), (d) (211) and (e) (204).

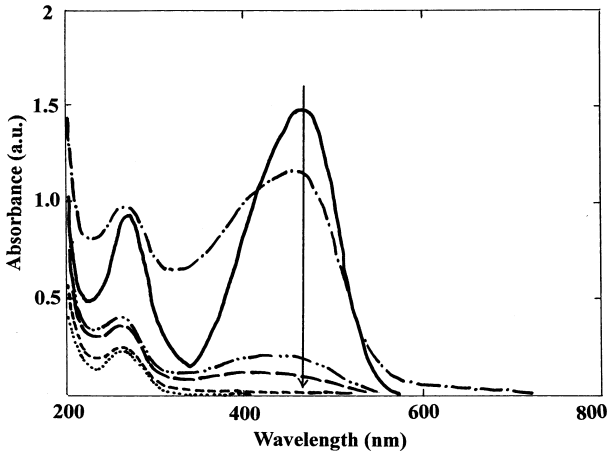

Figure 16 UV spectrum of Methyl Orange: Irradiation time (hr): (—) 0, (·····) 4, (—·—·) 8, (– – –)12, (------) 16, (·····) 20.

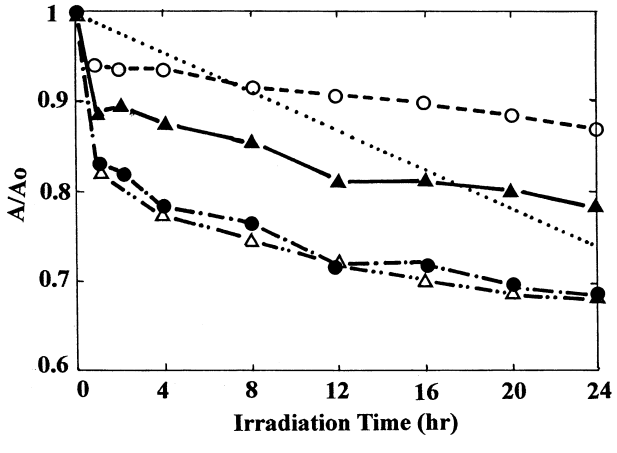

Figure 17 Photocatalytic activity of the helical TiO_2/CMC microtubes which was heat treated in N_2. Ao: UV intensity at the irradiation time of zero, A: UV intensity at some irradiation times. Heat-treatment temperature: (▲) 500°C, (△) 600°C, (●) 700°C, (○) 800°C, (------) commercial TiO_2.

be obtained at the heat-treatment temperature of 650°C.

The CMC can effectively absorb the EM waves of GHz regions to generate inductive microcurrent and thus micromagnetic field around the coils [47]. The coil diameter of the CMC is of the order of microns, and coil pitch and fiber diameter were in the nanometer orders. Accordingly, the CMC may also absorb EM waves of THz or PHz regions; up to visible light to violet right regions. It was found that the helical TiO_2/CMC microtubes had high photocatalytic activity, while helical TiO_2 microtubes without a core CMC had poor or no catalytic activity as shown in Figs 17 and 18. It is possible that the core CMC enhance the photocatalytic activity of TiO_2 by the induced micromagnetic field. The helical TiO_2 microtubes obtained by the calcination at 700°C were pulverized and the photocatalytic activity was examined to evaluate the effect of the helical structure. Fig. 19 shows the photocatalytic activity of the samples with and without pulverization of the helical TiO_2 microtubes obtained by the calcination at 650°C. It can be seen that the helical TiO_2 microtubes without pulverization show higher photocatalytic activity than the pulverized sample (powder-like TiO_2). Furthermore, Figs 17 and 18 show the difference of A/Ao between the helical TiO_2/CMC microtubes and helical TiO_2 microtubes without a core CMC obtained at the heat-treatment or calcination temperature of 700°C. It can be seen that the helical TiO_2/CMC microtubes with a core CMC show higher catalytic activity than that

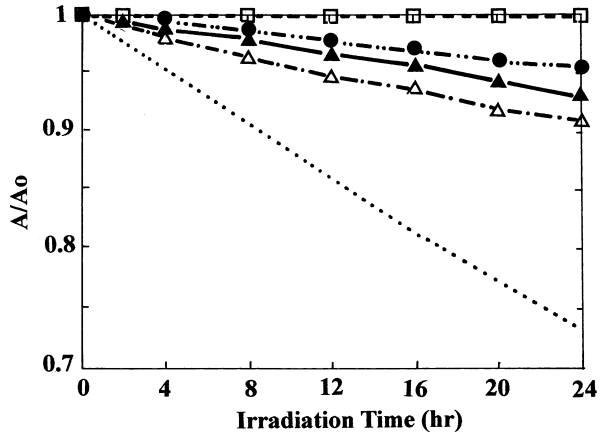

Figure 18 Photocatalytic activity of the helical TiO_2 microtubes without a core CMC. Caltination temperature in air: (△) 500°C, (▲) 650°C, (□) 800°C, (●) Pulverized TiO_2 microcoils obtained at calcination temperature of 650°C, (------) commercial TiO_2.

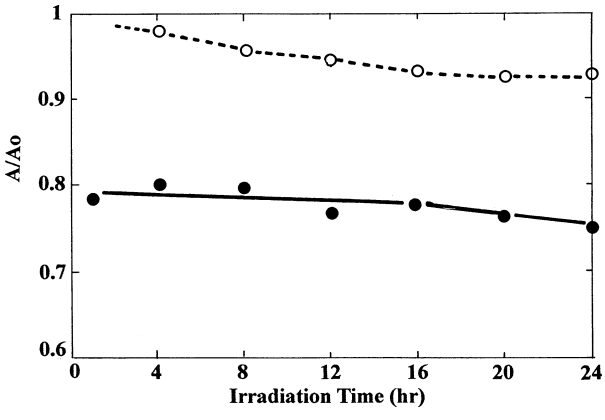

Figure 19 Difference of photocatalytic activity: (○) Difference of A/Ao between helical TiO_2 microtubes and pulverized helical TiO_2 microtubes obtained at a calcination temperature of 650°C. (●) Difference of A/Ao between the helical TiO_2/CMC microtubes obtained at a heat treatment temperature of 700°C and helical TiO_2 microtubes obtained at a calcination temperature of 700°C.

without a core CMC. These results suggest that the helical structure, especially of a core CMC activate and enhance the photocatalytic activity of the TiO_2.

4. Conclusions

Helical TiO_2/CMC (carbon microcoils) microtubes and pure helical TiO_2 microtubes without a core CMC were obtained by the TiO_2 layers coatings on the CMC templates using the sol-gel and chemical vapor deposition (CVD) processes using titanium tetra-isopropoxide as the Ti source. The preparation conditions, morphologies and photocatalytic activity were examined in detail. Using a sol-gel process, thin helical TiO_2 microcoils templated the grooves between two adjacent coils or helical TiO_2 microtubes with coiling patterns on the outer surface were obtained depending on the coating conditions. On the other hand, using a CVD process, helical TiO_2/CMC microtubes and pure helical TiO_2 microtubes without a core CMC with uniform thickness of TiO_2 (anatase) layers were obtained. The optimum gas flow rates for obtaining the TiO_2-coated CMC with uniform TiO_2 layers and with high yield were as follows; TIPO $= 6.4 \times 10^{-6}$ m^3/min, $H_2O = 1.39 \times 10^{-5}$ m^3/min, and total gas flow rate $= 1.6 \times 10^{-3}$ m^3/min. The helical TiO_2/CMC microtubes showed higher photocatalytic activity than that of commercial TiO_2 powder. It was considered that helical structure activated and enhanced the photocatalytic activity of TiO_2, probably caused by the generation of inductive micro electric current by the irradiation of UV light resulting in the generation of micromagnetic field around the tubes.

Acknowledgements

The authors thanks to Kazunori Nakano from Nagoya Municipal Industrial Research Institute in Japan for XRD measurements. This research was supported by Grant-in Aid for the Development of Innovative Technology (No. 13506) by The Ministry of Education, Culture, Sports, Science and Technology of Japan, as well as Japan Society for the Promotion of Science (P02372).

References

1. W. R. DAVIS, R. J. SLAWSON and G. R. RIGBY, *Nature* **171** (1953) 756.
2. J. GALUSZKA and M. H. BACK, *Carbon* **22** (1984) 141.
3. S. AMELINCKX, X. B. ZHANG, D. BERMAERTS, X. F. ZHANG, V. IVANOV and J. B. NAGY, *Science* **265** (1994) 635.
4. K. HERNADI, A. FONSECA, J. B. NAGY, D. BERNAERTS and A. A. LUCA, *Carbon* **34** (1996) 1249.
5. A. ADDAMIANO, *J. Cryst. Growth* **58** (1982) 617.
6. T.-K. KANG, S.-D. PARK, C.-K. RHEE and II.-H. KUK, in Proc. 5th Japan-Korea Ceramic Seminar (1989) p. 249.
7. S. MOTOJIMA, T. HAMAMOTO and H. IWANAGA, *J. Cryst. Growth* **158** (1996) 79.
8. S. MOTOJIMA, S. UENO, T. HATTORI and K. GOTO, *Appl. Phys. Lett.* **54** (1989) 1001.
9. S. MOTOJIMA, S. UENO, T. HATTORI and H. IWANAGA, *J. Cryst. Growth* **96** (1989) 383.
10. U. VOGT, H. HOFMANN and V. KRAMER, *Key Eng. Mater.* **89–91** (1994) 29.
11. S. MOTOJIMA, T. YAMANA, T. ARAKI and H. IWANAGA, *J. Electrochem. Soc.* **142** (1995) 3141.
12. H.-F. ZHANG, C.-M. WANG, E. C. BUCK and L.-S. WANG, *Nano Lett.* **3** (2003) 577.
13. K. SUGIYASU, S. TAMARU, M. TAKEUCHI, D. BERTHIER, I. HUC, R. ODA and S. SHINKAI, *Chem. Comm.* (2002) 1212.
14. J.-H. JUNG, Y. ONO and S. SHINKAI, *Chem. Eur. J.* **6** (2000) 9.
15. S. KOBAYASHI, N. HAMASAKI, M. SUZUKI, M. KIMURA, H. SHIRAI and K. HANABUSA, *J. Amer. Chem. Soc.* **124** (2002) 6550.
16. S. MOTOJIMA, M. KAWAGUCHI, K. NOZAKI and H. IWANAGA, *Appl. Phys. Lett.* **56** (1990) 321.
17. S. MOTOJIMA, M. HIRATA and H. IWANAGA, *J. Chem. Vapor Deposition* **3** (1994) 87.
18. S. MOTOJIMA, Y. ITOH, S. ASAKURA and H. IWANAGA, *J. Mater. Sci.* **30** (1995) 5049.
19. S. MOTOJIMA, S. ASAKURA, M. HIRATA and H. IWANAGA, *Mater. Sci. Eng.* B **34** (1995) L9.
20. S. MOTOJIMA, T. HAMAMOTO, N. UESHIMA, Y. KOJIMA and H. IWANAGA, *Electrochem. Soc. Proceedings* **97–25** (1997) 433.
21. S. MOTOJIMA, Y. KOJIMA, T. HAMAMOTO, N. UESHIMA and H. IWANAGA, *ibid.* **97–39** (1997) 595.

22. M. KAWAGUCHI, K. NOZAKI, S. MOTOJIMA and H. IWANAGA, *J. Cryst. Growth* **118** (1992) 309.
23. S. MOTOJIMA, S. YANG, X. CHEN and H. IWANAGA, *Mater. Res. Bull.* **35** (2000) 203.
24. S. MOTOJIMA, I. HASEGAWA, M. KAWAGUCHI, N. NOZAKI and H. IWANAGA, *J. Chem. Vapor Deposition* **1** (1992) 136.
25. S. MOTOJIMA, S. KAGIYA and H. IWANAGA, *J. Mater. Sci.* **31** (1996) 4641.
26. S. MOTOJIMA, H. ASANO and H. IWANAGA, *J. Eur. Ceram. Soc.* **16** (1996) 989.
27. S. MOTOJIMA, W. IN-HWANG and X. CHEN, *Mater. Res. Bull.* **35** (2000) 1517.
28. S. YANG, N. UESHIMA and S. MOTOJIMA, *J. Cryst. Growth* (accepted).
29. Y. HAMASAKI, S. OHKUBO, K. KURAKAMI, H. SEI and G. NOGAMI, *J. Electrochem. Soc.* **141** (1994) 660.
30. K. KAJIWARA and T. YAO, *J. Sol-Gel Sci. Technol.* **17** (2000) 239.
31. L. KAVAN and M. GRATZEL, *Electrochim. Acta* **40** (1995) 643.
32. M. DJ BLEGIC, Z. V. SAPONJIC, J. M. NEDELJKOVIC and D. P. USKOKOVIC, *Mater. Lett.* **54** (2002) 298.
33. L. KAVAN, B. O. REGAN, A. KAY and M. GRATZEL, *J. Electroanal. Chem.* **346** (1993) 291.
34. C. NATARAJIAN and G. NOGAMI, *J. Electrochem. Soc.* **143** (1996) 1547.
35. H. YIN, Y. WADA, T. KITAMURA, S. KAMBE, S. MURASAWA, H. MORI, T. SAKATA and S. YANAGIDA, *J. Mater. Chem.* **11** (2001) 1694.
36. H. CHENG, J. MA, Z. ZHAO and L. QI, *Chem. Mater.* **7** (1995) 663.
37. H. IMAI, Y. TAKEI, K. SHIMIZU, M. MATSUDA and H. HIRASHIMA, *J. Meter. Chem.* **9** (1999) 2971.
38. D. GONG, C. A. GRIMES, O. K. VARGHESE, W. HU, R. S. SINGH, Z. CHEN and E. C. DICKEY, *J. Mater. Res.* **16** (2001) 3331.
39. S. MOTOJIMA, T. SUZUKI, Y. NODA, A. HIRAGA, H. IWANAGA, T. HASHISHIN, Y. HISHIKAWA, S. YANG and X. CHEN, *Chem. Phys. Lett.* **378** (2003) 111.
40. S. MOTOJIMA, T. SUZUKI, Y. HISHIKAWA and X. CHEN, *Jpn. J. Appl. Phys.* **42** (2003) L938.
41. V. A. KARACHINOV, *Zhurnal Tekhnicheskoi Fiziki* **68** (1998) 133.
42. E. I. GIVARGIZOV and P. A. BABASIAM, *J. Crystal Growth* **37** (1977) 140.
43. R. A. BABASIAN and E. I. GIVARGIZOV, *J. Mater. Sci.* **15** (1980) 1619.
44. YA. E. GEGUZIN and N. N. OVCHARENKO, *Kristallografiya* **11** (1966) 272.
45. K. SHIBAGAKI, S. MOTOJIMA and M. HASHIMOTO, *Mater. Technol.* **18** (2000) 400.
46. R. J. BERRY and M. R. MUELLER, *Microchem. J.* **50** (1994) 28.
47. S. MOTOJIMA, Y. NODA, S. HOSHIYA and Y. HISHIKAWA, *J. Appl. Phys.* **94** (2003) 2315.

Received 26 August
and accepted 12 January 2004